

2011

Nanoconfinement of lithium borohydride in Cu-MOFs towards low temperature dehydrogenation

WW Sun

Fudan University

Shaofeng Li

Fudan University Shanghai

Jianfeng Mao

jm975@uow.edu.au

Zaiping Guo

University of Wollongong, zguo@uow.edu.au

Hua K. Liu

*University of Wollongong, hua_liu@uow.edu.au**See next page for additional authors*

Publication Details

Sun, W., Li, S., Mao, J., Guo, Z., Liu, H. K., Dou, S. Xue. & Yu, X. (2011). Nanoconfinement of lithium borohydride in Cu-MOFs towards low temperature dehydrogenation. *Dalton Transactions: an international journal of inorganic chemistry*, 40 (21), 5673-5676.

Authors

W.W Sun, Shaofeng Li, Jianfeng Mao, Zaiping Guo, Hua K. Liu, S. X. Dou, and Xuebin Yu

Cite this: *Dalton Trans.*, 2011, **40**, 5673

www.rsc.org/dalton

COMMUNICATION

Nanoconfinement of lithium borohydride in Cu-MOFs towards low temperature dehydrogenation†

Weiwei Sun,^a Shaofeng Li,^a Jianfeng Mao,^b Zaiping Guo,^{*b} Huakun Liu,^b Shixue Dou^b and Xuebin Yu^{*a,b}

Received 9th December 2010, Accepted 4th April 2011

DOI: 10.1039/c0dt01727b

Successful synthesis and investigation of a new material that uses copper-metal-organic frameworks (Cu-MOFs) as the template for loading LiBH₄ are reported. The nanoconfinement of LiBH₄ in the pores of Cu-MOFs results in an interaction between LiBH₄ and Cu²⁺ ions, enabling the LiBH₄@Cu-MOFs system to achieve a much lower dehydrogenation temperature than pristine LiBH₄.

Since hydrogen has been regarded as a future energy carrier of renewable energy, development of an efficient, robust, safe, and inexpensive hydrogen storage system is needed.¹ Metal borohydrides M(BH₄)_n with high hydrogen density have been attracting great interest as potential candidates for advanced hydrogen storage materials.² Among them, lithium borohydride (LiBH₄), a promising hydrogen storage material, is commercially available and has extremely high theoretical hydrogen capacity (18.3 wt.%, 121 kg m⁻³), but its practical application as a hydrogen storage material is limited due to the high gas-evolution temperature (about 380 °C).³ Many efforts have been made, with considerable progress, in solving the above-mentioned issues.⁴ For example, the employment of metals, metal halides, oxides, or metal hydrides as catalysts/dopants has been demonstrated to be an appropriate approach to reduce the operating temperature of metal borohydrides.⁵

On the other hand, a recent encouraging approach towards modifying the hydrogen storage properties of LiBH₄ has been mainly focused on the identification of nanostructural or porous materials as templates, such as carbon nanotubes, carbon fibers, mesoporous silica, and mesoporous carbon, which provides a strong nanoconfinement effect.⁶ For example, the confinement of LiBH₄ in ordered mesoporous SiO₂ (SBA-15)^{6a} and in highly ordered nanoporous hard carbon (NPC)^{6b} have resulted in significant reduction of the onset desorption temperature. Since metal-organic frameworks (MOFs), which have highly ordered and inherently understandable crystalline lattices, have been used for gas storage, they have become an attractive alternative to the traditional templates for hydrogen storage.⁷ It has been

widely demonstrated that MOFs are very effective templates for loading hydrogen storage materials, *e.g.* ammonia borane (AB) and NaAlH₄, to achieve improved kinetics and thermodynamics in hydrogen release.⁸ With these in mind, we selected a kind of Cu-MOFs (HKUST-1) as the template for loading LiBH₄ to clarify the effects of nanoconfinement on the dehydrogenation.

The metal-organic framework template used in this work, HKUST-1 [Cu₃(BTC)₂(H₂O)₃, BTC = benzene tricarboxylate], which was prepared according to a procedure in the literature,⁹ has small pore openings with a size of 9 Å × 9 Å and can be thermally stable up to 250 °C. The Cu₃(BTC)₂(H₂O)₃ sample was heated at 100 °C for six hours under vacuum to remove the coordinated water molecules to yield dehydrated Cu-MOFs, and the X-ray diffraction (XRD) results are compared in the ESI (Fig. S1†). Taking account of the good solubility of LiBH₄ in ether, dehydrated Cu-MOFs were mixed with an ether solution of LiBH₄ to achieve uniform dispersion and contact, which are indispensable for solid phase reactions. After ultrasonic treatment for ten minutes, the suspension was kept under vacuum for three hours at room temperature to remove the solvent and thus obtain the target compound, LiBH₄@Cu-MOFs.

The XRD patterns of pristine LiBH₄, dehydrated Cu-MOFs, and LiBH₄@Cu-MOFs before and after dehydrogenation are shown in Fig. 1. After loading, the peaks assigned to Cu-MOFs were still retained with only a slight shift (Fig. 1c), indicating

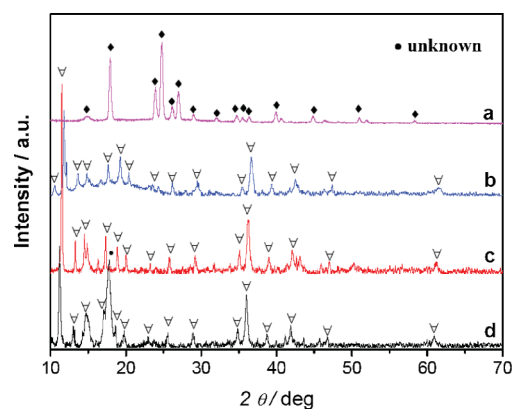


Fig. 1 Powder X-ray diffraction patterns of pristine LiBH₄ (a), dehydrated Cu-MOFs (b), LiBH₄@Cu-MOFs (c), and LiBH₄@Cu-MOFs dehydrogenated to 200 °C (d). (Characteristic peaks assigned to LiBH₄ and MOFs are marked by the symbols ◆ and ▽, respectively.)

^aDepartment of Materials Science, Fudan University, Shanghai, 200433, China. E-mail: yuxuebin@fudan.edu.cn; Tel: 86-21-55664581

^bInstitute for Superconducting and Electronic Materials, University of Wollongong, NSW 2522, Australia. E-mail: zguo@uow.edu.au

† Electronic supplementary information (ESI) available: Experimental details, results of XRD, DSC, XPS, BET, and density measurements. See DOI: 10.1039/c0dt01727b

that the sample has maintained its structural integrity. No peaks corresponding to LiBH_4 were found for the $\text{LiBH}_4@$ Cu-MOFs sample (Fig. 1c), indicating a successful loading of LiBH_4 into the pores of the MOFs. To obtain further evidence that LiBH_4 was well absorbed inside the Cu-MOFs, we compared the volume of pores and the surface area of Cu-MOFs before and after loading by means of Brunauer–Emmett–Teller (BET) measurements, and the results are shown in Fig. S2.† The N_2 adsorption and desorption of Cu-MOFs at 77 K shows the characteristics of a microporous material, while for $\text{LiBH}_4@$ Cu-MOFs, the measurement shows non-porous characteristics, suggesting the possibility of successful incorporation of LiBH_4 into the Cu-MOFs-pores or that the openings in Cu-MOFs were blocked by the LiBH_4 molecules. Further density measurements (ESI†) revealed that LiBH_4 had achieved loading into pores with a filling rate of 84 wt.%, while there was still 16 wt.% LiBH_4 left outside.

As shown in the temperature-programmed desorption (TPD) curves in Fig. S3,† the dehydrogenation of $\text{LiBH}_4@$ Cu-MOFs started from around 60 °C, which is dramatically lower than for the pristine LiBH_4 (380 °C). After heating up to 200 °C, a total gas release of 0.0048 mol g^{-1} was observed for the $\text{LiBH}_4@$ Cu-MOFs sample, which indicated partial decomposition of loaded LiBH_4 below this temperature (0.007 mol g^{-1} for a complete decomposition of the confined LiBH_4 to H_2).

Mass spectrometry (MS) was used to investigate the temperature profiles of volatile products released from $\text{LiBH}_4@$ Cu-MOFs samples. As shown in Fig. 2a, the $\text{LiBH}_4@$ Cu-MOFs sample started to release H_2 ($m/z = 2$) at around 75 °C, with the peak temperature at 110 °C, while the small peak at 265 °C should be regarded as the phase transition point of LiBH_4 .¹⁰ The H_2 -release peak temperature of the MS spectra was a little different from that of the TPD spectra (Fig. S3†), and the main reason would be that mass spectrometry was conducted under N_2 atmosphere, while TPD was conducted under an Ar/H_2 atmosphere. Accompanying the evolution of H_2 , the release of diborane ($m/z = 27$) occurred almost at the same starting and peak temperatures as H_2 , but was only revealed by a shoulder peak around 205 °C. By combination of the volumetric and gravimetric results, it is determined that the molar ratio of H_2 to diborane in the evolved gas is 20:1. It is well known that more stable metal borohydrides decompose at higher temperature and release mainly hydrogen, while less stable ones would desorb at lower temperatures and release considerable amounts of diborane by-product.^{11a} This effect is mainly due to the nature of diborane,

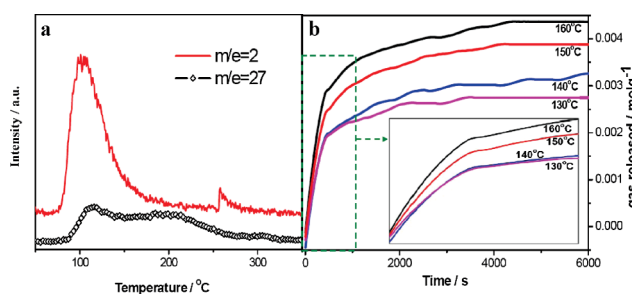


Fig. 2 MS signals of $\text{LiBH}_4@$ Cu-MOFs (a) and the time dependence of the first-step H_2 release plotted for loaded $\text{LiBH}_4@$ Cu-MOFs at different temperatures (b). The inset in (b) is an enlargement of the dehydrogenation time from 0 to 1000 s.

which is reported to decompose at about 250 °C by thermal decomposition and is not observed as a decomposition product at higher temperature. As reported previously in the literature,¹¹ during the decomposition of LiBH_4 , decreasing the desorption temperature could lead to the emission of diborane, which would accelerate the further decomposition of the remaining LiBH_4 . Therefore, in our study, the release of diborane may also result from the low decomposition temperature of LiBH_4 . The differential scanning calorimetry (DSC) result (Fig. S4†) shows a strong endothermic peak for this dehydrogenation, indicating that the dehydrogenation of $\text{LiBH}_4@$ Cu-MOFs is thermodynamically irreversible. To investigate the distinctly enhanced kinetics of this compound, the time-dependence of the first step dehydrogenation for loaded $\text{LiBH}_4@$ Cu-MOFs was measured over a temperature range from 130 to 160 °C, and the results are given in Fig. 2b. In order to exhibit clearly the different rates of the plots, the time-dependence plots in the range of 0–1000 s were enlarged and are shown in the inset of Fig. 2b. With increasing temperature, the amount of released gas was significantly increased, and the dehydrogenation kinetics was accelerated.

The XRD pattern of the loaded $\text{LiBH}_4@$ Cu-MOFs after dehydrogenation shows no change in the structure of the Cu-MOFs (Fig. 1d), which is also confirmed by the Fourier transform infrared (FT-IR) results (Fig. S5†), indicating the stability of the Cu-MOFs before and after dehydrogenation. However, a strong new peak at $2\theta = 17.8^\circ$ can be observed for the dehydrogenated sample, suggesting the formation of a new substance. To explore further details of the decomposition process, solid ^{11}B NMR measurements for the samples before and after dehydrogenation to 200 °C were conducted, as shown in Fig. 3. In the case of the sample before dehydrogenation, the strong peak with the chemical shift of -41.3 ppm could be assigned to the boron atoms in tetrahedral BH_4^- groups of LiBH_4 ,¹² and the much weaker one around 0.19 ppm could be attributed to the slight decomposition of LiBH_4 that may occur under the ultrasonic treatment. After dehydrogenation, the peak for the BH_4^- group still exists due to the residual undecomposed LiBH_4 (16 wt.%) on the outside surface of the Cu-MOFs pores, as demonstrated by BET results. Meanwhile, a strong peak at 0.19 ppm appeared after dehydrogenation to 200 °C, which could be assigned to the oxidative product of LiBH_4 , boric acid.¹³

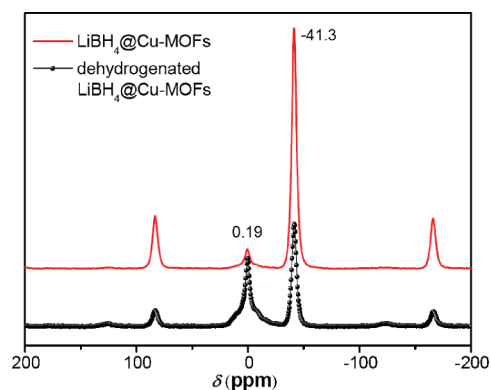


Fig. 3 ^{11}B NMR results for as-prepared $\text{LiBH}_4@$ Cu-MOFs before and after dehydrogenation at 200 °C. The two pairs of peaks (± 125 ppm and 83.9/–165.6 ppm) are regarded as the spinning side bands corresponding to the 0.19 and -41.3 ppm peaks, respectively.

In order to clarify the formation of boric acid in the loaded LiBH_4 @Cu-MOFs during decomposition, X-ray photoelectron spectroscopy (XPS) of Cu element was conducted, as shown in Fig. S6.† The $\text{Cu}2\text{p}_{2/3}$ binding energies shifted from 934 eV for dehydrated Cu-MOFs to 933 eV (loaded sample) and 932.5 eV (dehydrogenated sample), confirming a slight change in the coordination environment of Cu atoms, that is, the Cu atoms changed from divalent to mono- or even zerovalent, indicating that a redox reaction had occurred between LiBH_4 and the Cu^{2+} ions in the Cu-MOFs during decomposition. Given that the product of boric acid in the decomposed LiBH_4 @Cu-MOFs is quite similar to that of LiBH_4 oxidized by water molecules, a sample with LiBH_4 loaded into hydrated Cu-MOFs (LiBH_4 @Cu-MOFs- H_2O) was synthesized and analysed for comparison. Interestingly, it was found that the LiBH_4 @Cu-MOFs- H_2O sample showed evident hydrogen release during the loading process, indicating that the coordinated water molecules (one per Cu^{2+} ion) in the skeleton of the Cu-MOFs could react with LiBH_4 at room temperature, which opens up a research frontier on the controllable ambient temperature hydrolysis of metal borohydrides by using hydrated MOFs. The ^{11}B NMR result (Fig. S7†) on LiBH_4 @Cu-MOFs- H_2O indicated the formation of boric acid, with peaks appearing at around 0.19 ppm, again confirming the redox reaction in the LiBH_4 @Cu-MOFs system, while the presence of the peak at -41 ppm, corresponding to LiBH_4 , suggests that the residual LiBH_4 on the outside surface of the Cu-MOFs did not react with the H_2O in the hydrated MOFs as well. The above results indicate that LiBH_4 could dehydrogenate at low temperature through a redox reaction with Cu-O units or H_2O in the Cu-MOFs. However, this reaction only occurs for the LiBH_4 confined in the pores of MOFs.

For a better understanding of the reaction between LiBH_4 and Cu^{2+} ions after nanoconfinement, the schematic diagram in Fig. 4 was drawn to give an impression of the architecture: one LiBH_4 molecule is trapped per Cu^{2+} ion inside the “pore” of the Cu-MOFs, and the interaction between LiBH_4 and the Cu^{2+} ions is expressed by the dotted lines. Given the small pore size with diameter of 0.9 nm, the interaction may become easier between the LiBH_4 and Cu^{2+} ions after loading. In addition, after removal of the coordinated water molecules, the active coordination sites

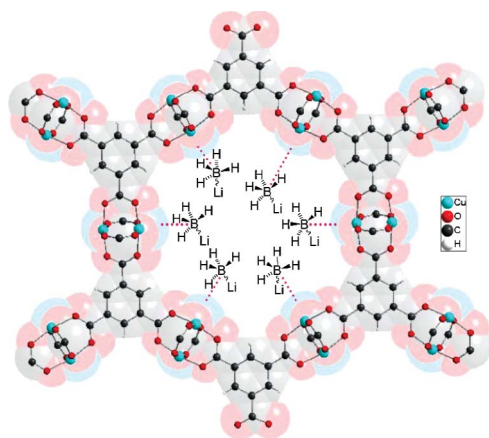


Fig. 4 Schematic diagram of LiBH_4 molecules loaded into the pores of Cu-MOFs. (The interaction between the LiBH_4 and the Cu^{2+} ions is indicated by the dotted lines.)

of copper atoms that exist in the dehydrated Cu-MOFs could further promote the interaction. The above hypothesis can be confirmed by a direct mixing of LiBH_4 and Cu-MOFs, in which only a trace of gas evolution was observed on heating the sample to 200 °C (Fig. S4†). Therefore, nanoconfinement of LiBH_4 in the pores of MOFs is a crucial factor for igniting the redox reaction between LiBH_4 and Cu-O units, which could achieve superior dehydrogenation properties in this system compared to other LiBH_4 systems with oxide dopants.^{5a,5c}

In conclusion, we have selected a special kind of Cu-MOFs as the template for loading LiBH_4 to produce a possible hydrogen storage material. The confinement by nanostructural materials and the consequent redox reaction between LiBH_4 and Cu-O units enabled dehydrogenation to occur in LiBH_4 @Cu-MOFs at a much lower dehydrogenation temperature. Such nanoconfinement could be widely used in cooperation with other positive effects, such as: redox, catalysis, or hydrolysis reactions, to achieve the potential for hydrogen storage materials with vastly improved dehydrogenation.

Acknowledgements

This work was partially supported by the National Natural Science Foundation of China (Grant No. 51071047), the Program for New Century Excellent Talents in Universities (NCET-08-0135), the Australian Research Council (DP0878661), and the PhD Programs Foundation of the Ministry of Education of China (20090071110053). We thank Dr Tania Silver for her critical reading of this paper.

Notes and references

- (a) W. Grochala and P. P. Edwards, *Chem. Rev.*, 2004, **104**, 1283; (b) M. S. Dresselhaus and I. L. Thomas, *Nature*, 2001, **414**, 332; (c) L. Schlappbach and A. Züttel, *Nature*, 2001, **414**, 353; (d) Y. F. Liu, K. Zhong, K. Luo, M. X. Gao, H. G. Pan and Q. D. Wang, *J. Am. Chem. Soc.*, 2009, **131**, 1862.
- (a) S. I. Orimo, Y. Nakamori, J. R. Eliseo, A. Züttel and C. M. Jensen, *Chem. Rev.*, 2007, **107**, 4111; (b) P. Edwards, W. Grochala, D. Book, I. R. Harris, *International Patent* WO2004096700, 2004; (c) H. W. Li, K. Kikuchi, Y. Nakamori, K. Miwa, S. Towatab and S. Orimo, *Scripta Mater.*, 2007, **57**, 679.
- (a) E. M. Fedneva, V. L. Alpatova and V. I. Mikheeva, *Russ. J. Inorg. Chem. (Transl. of Zh. Neorg. Khim.)*, 1964, **9**, 826; (b) A. Züttel, P. Wenger, S. Rentsch, P. Sudan, Ph. Mauron and Ch. Emmenegger, *J. Power Sources*, 2003, **118**, 1.
- (a) J. J. Vajo and G. L. Olson, *Scripta Mater.*, 2007, **56**, 829; (b) M. Aoki, K. Miwa, T. Noritake, G. Kitahara, Y. Nakamori, S. Orimo and S. Towata, *Appl. Phys. A: Mater. Sci. Process.*, 2005, **80**, 1409; (c) G. P. Meisner, M. L. Scullin, M. P. Balogh, F. E. Pinkerton and M. L. Meyer, *J. Phys. Chem. B*, 2006, **110**, 4186; (d) G. Barkhordarian, T. Klassen and R. Bormann, *J. Phys. Chem. B*, 2006, **110**, 11020.
- (a) X. B. Yu, D. M. Grant and G. S. Walker, *Chem. Commun.*, 2006, 3906; (b) Y. H. Guo, X. B. Yu, L. Gao, G. L. Xia, Z. P. Guo and H. K. Liu, *Energy Environ. Sci.*, 2010, **3**, 465; (c) X. B. Yu, D. A. Grant and G. S. Walker, *J. Phys. Chem. C*, 2008, **112**, 11059; (d) J. J. Vajo and S. L. Skeith, *J. Phys. Chem. B*, 2005, **109**, 3719.
- (a) P. Ngene, P. Adelhelm, M. B. Andrew, K. P. de Jong and P. E. de Jongh, *J. Phys. Chem. C*, 2010, **114**, 6163; (b) X. F. Liu, D. Peaslee, C. Z. Jost and E. H. Majzoub, *J. Phys. Chem. C*, 2010, **114**, 14036; (c) A. F. Gross, J. J. Vajo, S. L. Van Atta and G. L. Olson, *J. Phys. Chem. C*, 2008, **112**, 5651.
- (a) N. L. Rosi, J. Eckert, M. Eddaoudi, D. T. Vodak, J. Kim, M. O’Keeffe and O. M. Yaghi, *Science*, 2003, **300**, 1127; (b) J. L. C. Rowsell and O. M. Yaghi, *Angew. Chem., Int. Ed.*, 2005, **44**, 4670; (c) B. Chen, N. W. Ockwig, A. R. Millward, D. S. Contreras and O. M. Yaghi, *Angew. Chem., Int. Ed.*, 2005, **44**, 4745.

- 8 (a) Z. Y. Li, G. S. Zhu, G. Q. Lu, S. L. Qiu and X. D. Yao, *J. Am. Chem. Soc.*, 2010, **132**, 1490; (b) R. K. Bhakta, J. L. Herberg, B. Jacobs, A. Highley, R. Behrens, Jr., N. W. Ockwig, J. A. Greathouse and M. D. Allendorf, *J. Am. Chem. Soc.*, 2009, **131**, 13198.
- 9 (a) S. S. Y. Chui, M. F. L. Samuel, J. P. H. Charmant, A. G. Orpen and I. D. Williams, *Science*, 1999, **283**, 1148; (b) K. Schlichte, T. Kratzke and S. Kaskel, *Microporous Mesoporous Mater.*, 2004, **73**, 81.
- 10 H. I. Schlesinger and H. C. Brown, *J. Am. Chem. Soc.*, 1940, **62**, 3429.
- 11 (a) O. Friedrichs, A. Remhof, S. J. Hwang and A. Züttel, *Chem. Mater.*, 2010, **22**, 3265; (b) O. Friedrichs, A. Borgschulte, S. Kato, F. Buchter, R. Gremaud, A. Remhof and A. Züttel, *Chem.–Eur. J.*, 2009, **15**, 5531.
- 12 (a) S. J. Hwang, R. C. Bowman, Jr., J. W. Reiter, J. Rijssenbeek, G. L. Soloveichik, J. C. Zhao, H. Kabbour and C. C. Ahn, *J. Phys. Chem. C*, 2008, **112**, 3164; (b) M. Au, A. R. Jurgensen, W. A. Spencer, D. L. Anton, F. E. Pinkerton, S.-J. Hwang, C. Kim and R. C. Bowman, Jr., *J. Phys. Chem. C*, 2008, **112**, 18661.
- 13 R. L. Corey, D. T. Shane, R. C. Bowman, Jr. and M. S. Conradi, *J. Phys. Chem. C*, 2008, **112**, 19784.